EVOLUTION IN ELECTRICAL AND ELECTRONIC ENGINEERING
e-ISSN: 2756-8458

EEEE

Vol. 6 No. 1 (2025) 76-84
https://publisher.uthm.edu.my/periodicals/index.php/eeee

Efficiency Investigation of a Four-Segment Permanent Magnet Flux Reversal Motor Design

Muhammad Hakim Zam Telani[1], Mahyuzie Jenal[1]*

[1] *Department of Electrical Engineering, Faculty of Electrical and Electronic Engineering, University Tun Hussein Onn Malaysia, 86400 Parit Raja, Johor, MALAYSIA*

*Corresponding Author: mahyuzie@uthm.edu.my
DOI: https://doi.org/10.30880/eeee.2025.06.01.010

Article Info

Received: 15 January 2025
Accepted: 24 April 2025
Available online: 9 May 2025

Keywords

Flux Reversal Machine (FRM), Permanent Magnet (PM), Segmented Stator Flux Reversal Machine (SSFRM), JMAG Designer 18.1, Finite Element Analysis (FEA)

Abstract

The paper focuses on the segmented stator Flux Reversal Motor (FRM). It lists some critical optimization difficulties which include flux leakage and cogging torque, with an objective of improving the efficiency through use of Finite Element Analysis (FEA). Building on what is already known regarding the operation of flux reversal and permanent magnet machines the paper examines new design features such as segmental stators to said matters of faults and torque. These insights provide a framework as a basis for designing the proposed FRM. A scientific procedure was used for designing and simulating the motor with the help of JMAG Designer 18.1. These were followed by several basic parameters such as parameter specification, geometry modification, material determination, and other performance checks. Closely related with pm synchronous motors, the analyses of the relationship between torque, flux linkage, and efficiency to set up design parameters. Using performance evaluation, the design of the 12-stator-slot, 16-pole SSFRM yielded a peak torque of 43.05 Nm with a power output of 22.24 kW. Although the design revealed stable flux interaction and ability to handle faults, the design absorbed a very high amount of copper losses (39.68 kW) thereby limiting its efficiency to 50.8 %. This points to the problem of optimisation, now, especially with the focus on the magnetic and material quality. In turn, the overall potential of the SSFRM for energy efficient applications is presented, with the segmental stator appearance giving it significant possibilities. However, increasing efficiency and minimising losses has to be achieved, in order to make its real-life application and commercial utilization.

1. Introduction

The Permanent Magnet Flux Reversal Motors (PMFRMs) are electric machine classifications which employ reversible stator magnetic field to develop high density torque and efficient speed. Comparing PM FRMs to more traditional permanent magnet motors, the latter is characterized by a flux-reversal system which provides improved capability to withstand the high torque loads while maintaining compact sizes. This motor topology is particularly attractive for use in those application areas that demand a high-power density, high reliability, and very low level of maintenance [1]. The proposed method to achieve enhanced PM FRM performance is by employing a segmented stator structure. Segmented stators produce less manufacturing and assembling costs while individual segments can be produced to produce slight desired changes in magnetic responses of the motor. However, this leads to some specific difficulties related to magnetizing the structure in segments, as well as minimizing magnetic field leakage and energy losses [2].

Evolution in Electrical and Electronic Engineering Vol. 6 No. 1 (2025) p. 76-84

1.1 Problem Statement

An essential factor is an identification of some appropriate geometric parameters for the functioning, elements, as well as an optimal ratio between the performance and energy consumption. Embedded in the structure is additional design challenges as far as magnetic flux distribution and structural implementation is concerned. In JMAG 2D Finite Element Analysis (FEA) it is crucial to accurately model the geometry of the motor to achieve optimum values of flux density, Torque ripple and thermal characteristics of the motor. The segmented stator structure traditionally amplifies this factor because microcogging is manifested by inherent magnetic asymmetry and can lead to performance deterioration and lower efficiency. FEA tools are very important in evaluating the motor performance and in quantifying the cogging torque and determining mitigation measures such as pole slot harmonics, and magnet position. Moreover, the procedure of obtaining high efficiency in the PM FRM design involves paying attention to iron and copper losses since they consume most energy.

2. Literature Review

2.1 Flux Reversal Motor (FRM)

The FRM has been presented as a way to retain the benefits of both switched-reluctance and PM machines. Having PMs on the stator makes the FRM a machine that stands out twice. As the rotor travels, the PM flux linkage in the stator phase concentration coils switches polarity [3]. It is affordable and appropriate for mass manufacturing due to its straightforward construction. Due to its low mutual and self-inductances, it has a high fault tolerance and a low electrical time constant [3]. With these benefits, the FRM may be able to play a significant role in automobile generators. But because of its structure, there is a noticeable PM flux leakage (fringing). The power density and torque constant of the FRM are negatively impacted by this flux leakage.

2.2 Torque Performance Analysis of Three-Phase Flux Reversal Machines

FRM shown in Figure 1 have similar magnetic structures with the switched reluctance machines, but multipole PM mounted on or inserted into each stator teeth. The no-load flux linkage of the three-phase windings reverses its polarity when the rotor travels by a slot pitch [4]. Thus, it is called “flux reversal.” FRMs have been widely applied in both low-speed and high-speed areas due to their superior properties [5]. For example, FRM was recognized as a promising candidate for electric vehicle propulsion because of its simple rotor configuration, low time constant, and fast transient response [6]– [9]. Moreover, since the rotation of winding flux linkage is much faster than that of the rotor, FRM can produce a large torque at the low-speed operation. Hence, FRMs have also been used in direct-drive servo applications [10] and wind-power generations [11].

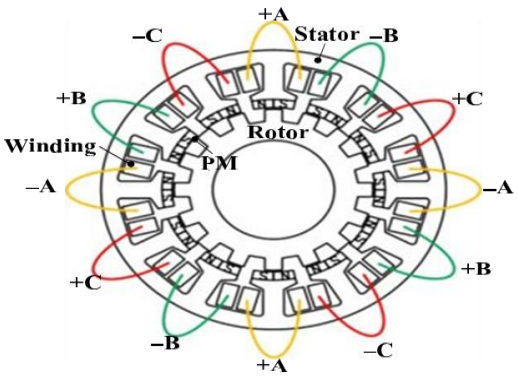

Fig. 1 *Configuration of a 12-stator-slot/16-rotor-slot FRM*

2.3 Parameter Effect on Torque Performances

The influences of rotor slot number, split ratio, PM thickness, stator and rotor slot opening ratio on the torque performances including average torque, cogging torque, and ripple torque are investigated using the derived expressions. Since the ratio of stator slot number to rotor slot number of three-phase FRMs is usually chosen around 3/4 in literatures, the 12-stator-slot FRMs having 13-, 14-, 16-, 17-, and 19-rotor slot are selected for analysing the effect of rotor slot number on torque performances. In order to have a reasonable study, some key parameters such as stator outer diameter, stack length, heat loading, and others are kept the same for these models. Their electromagnetic parameters are listed in Table 1.

Table. 1 *Parameters of the three-phase FRM models [4]*

Parameter	Value	Parameter	Value
Stator outer diameter	170 mm	Stack length	100 mm
Stator slot number	12	Airgap length	0.5 mm
Series turns per phase	80	Winding pitch	1
Heat loading	1100 A/cm∗A/mm^2	Rotation speed	600 r/min
PM permeability	1.068	Phase current	19.4 A
PM remanence	1.21 T	Slot fill factor	0.5

3. Methodology

For the methodology, this section outlines the methodology employed to accomplish the first and second objectives of the study. The primary goals are to propose and design good geometries parameter that suitable in FRM with segmented structure and analyze the motor's performances and efficiency under various operational loads. When introducing a new structure, it is imperative to conduct tests to ascertain the smooth operation of the motor. The process commences with the systematic sketching of each motor part in the geometry editor, followed by further development in the designer. In the designer, materials and conditions are specified for subsequent analysis and simulation. This step-by-step approach ensures a comprehensive exploration of the motor's design and performance characteristics.

3.1 Parameter and Materials

The table below shows the design parameters of a stator and rotor, likely for a segmented stator FRM. Separated into Table 2 and Table 3, the table details specifications like the number of poles and slots, radius measurements, and material types. This information provides a clear picture of the design choices made for the stator and rotor in this segmented stator FRM.

Table 2 *Parameter of the proposed rotor and stator*

Parameter	Value
Stator poles	12
Stator slots	12
Rotor poles	16
Outer radius of stator, (mm)	132
Inner radius of stator, (mm)	95.9
Outer radius of rotor, (mm)	92.4
Inner radius of rotor, (mm)	62.4
Airgap length, (mm)	0.5
Motor stack length, (mm)	70
Revolution per minute (rpm)	1200

Table 3 *Materials and Condition*

Part	Material	Condition
Rotor	Nippon Steel 35H210	Motion: rotation Torque: nodal force
Stator	Nippon Steel 35H210	-
Armature Coil	Conductor Copper	FEM Coil
Permanent Magnet	Neomax-P8H (irreversible) Magnetization pattern: Circumferential Anisotropic Pattern	-

3.2 System Flowchart of Overall Project

This section outlines the methodology employed to accomplish the first and second objectives of the study. The primary goals are to propose a propose and design good geometries parameter that suitable in FRM with segmented structure and analyze the motor's performances and efficiency under various operational loads.

Evolution in Electrical and Electronic Engineering Vol. 6 No. 1 (2025) p. 76-84

When introducing a new structure, it is imperative to conduct tests to ascertain the smooth operation of the motor. The process commences with the systematic sketching of each motor part in the geometry editor, followed by further development in the designer. In the designer, materials and conditions are specified for subsequent analysis and simulation. This step-by-step approach ensures a comprehensive exploration of the motor's design and performance characteristics.

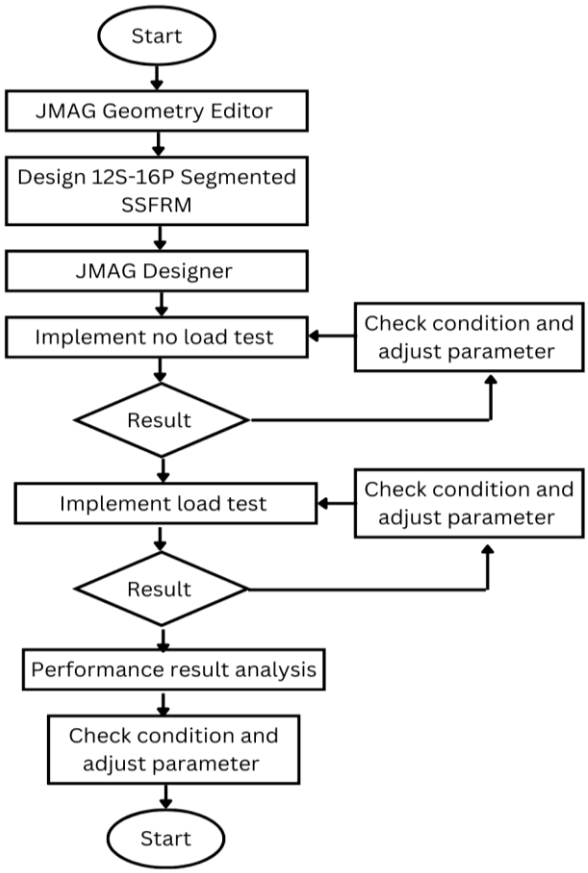

Fig. 2 *Overall implementation of the study*

3.3 Formula Use in Simulation

This section likely presents formulas used in JMAG Designer software for defining coil properties and simulation settings. Equations (1), (2), and (3) might be related to calculating the number of turns needed for a coil in motor design, influencing factors like magnetic field strength. Equations (4) and (5) seem to focus on simulation control. Equation (4) might help determine the total simulation time, while equation (5) might be used to calculate frequencies relevant to analyzing motor behavior under various operating conditions. While JMAG Designer offers functionalities to handle these calculations based on user input, understanding the underlying formulas (e.g., effective area, number of turns per layer, coil area, end time, and frequency) can provide valuable insights into your motor design and simulation setup.

$$N_a = \frac{A_{eff}}{A_{coil}} \tag{1}$$

$$A_{eff} = A(0.5) \tag{2}$$

$$A_{coil} = \pi(0.5^2) \tag{3}$$

$$t_e = \frac{1}{f_e} \tag{4}$$

$$f_e = \frac{n.N_r}{60} \tag{5}$$

3.4 Circuit Setting

All armature coils must be linked to the appropriate FEM coil in the next stage, which is the coil construction shown in Figure 3. The machine's circuit is included in the magnetic transient model. In this section, twelve FEM coils are connected into the armature coil in a parallel configuration with a grounding once the circuit has been added. The circuit's U, V, and W three-phase coils need to be finalized. The circuit for the U, V, and W tests differs from that of the twelve and six coil tests. Therefore, each coil that is connected to the FEM coil in the condition setting needs to be examined.

$$Number\ of\ Turn = \frac{Area\ of\ effect}{Area\ of\ coil} \tag{6}$$

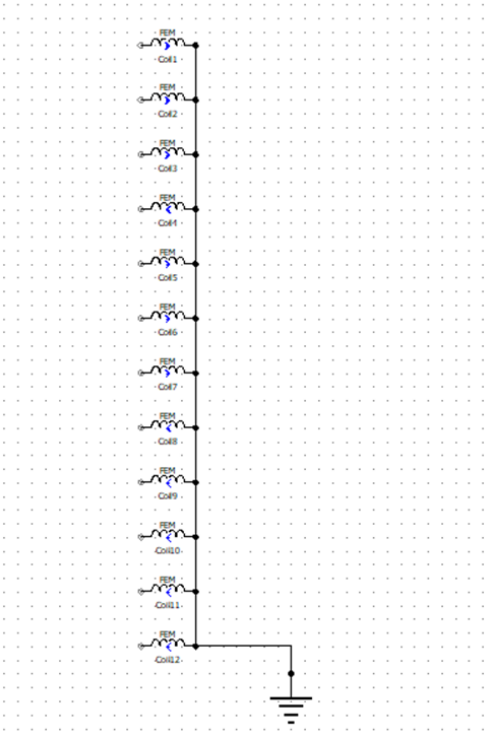

Fig. 3 *Circuit arrangement of FEM coil for single phase*

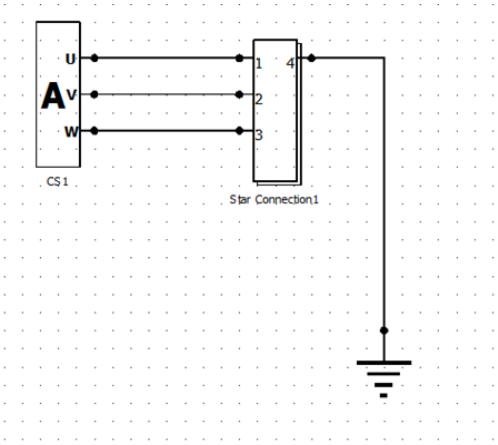

Fig. 4 *Circuit arrangement of FEM coil for three phases*

4. Result and Discussion

For purposes of this analysis, it is necessary to assume constant permanent magnet flux linkage and zero armature current density during no load test. This makes it possible to study the maximum limit of magnetic flux that may be applied as well as the pattern of its distribution in the motor. Other angles investigated also include cogging torque and back EMF. Motor performance under different loads is evaluated by analyzing results from load tests. It can effectively imitate the practice of increasing the armature current density from zero to a certain practice, for instance, 30 arms/mm2. The load condition of the motor is determined by analyzing such factor as torque, power, speed, loss, and efficiency among others. Additional load tables that include the peak and RMS armature currents of the suggested design are incorporated into the software for further load analysis.

4.1 Flux Linkage Analysis

A coil test procedure was used to analyze the flux linkage in order to identify the distinct flux linkage patterns produced by each armature coil and assess the properties of these linkages. The armature coils have a set polarity and wind in a clockwise manner. The PM, on the other hand, alternate between each other and are oriented in opposite orientations. Tests are conducted on the coil flux linkage when the motor is operating at 1200 rpm. Fig. 6, graphically represent the coil test results for this segmented stator FRM.

Evolution in Electrical and Electronic Engineering Vol. 6 No. 1 (2025) p. 76-84

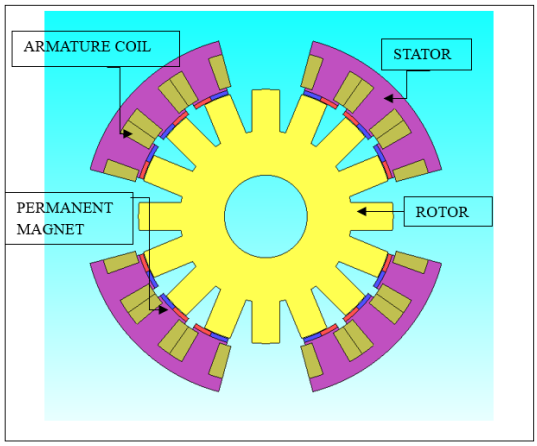

Fig. 5 *Proposed design of 12S-16P FRM*

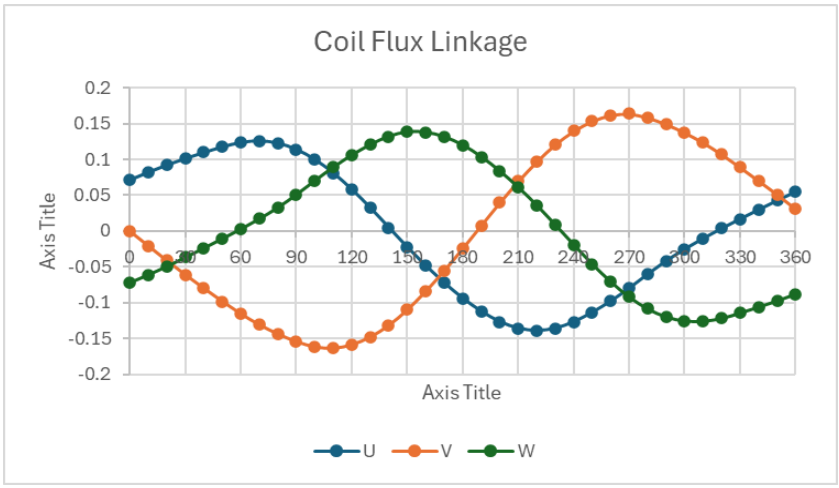

Fig. 6 *Graph of coil flux linkage proposed design*

4.2 Cogging Torque

Cogging torque is practically the outcome of a delicate interplay between the rotor's PM and stator slots. This procedure may in fact be destabilizing to the entire motor structure due to the introduction of other adverse effects such as noise, vibration, resonances, and speed ripple. Fig. 7 provides a visual representation of the cogging torque for the proposed designs FRM. The figure shows that, for suggested design, the cogging torque for the no load test has a peak-to-peak value of 20.8588 Nm at 300 degrees at the highest and -23.7544 Nm at 40 degrees at the lowest. The motor will vibrate at its peak cogging torque, and its performance increases with the least cogging torque.

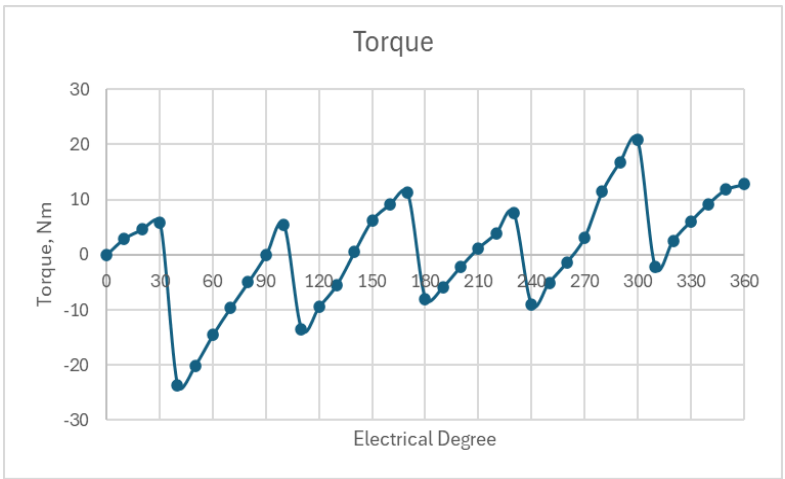

Fig. 7 *Graph of cogging torque of proposed design SSFRM*

4.3 Load Analysis

SSFRM motor performance at load test condition can be determined when varying Ja specific armature current density and Je specific field excitation coil density from 0 $Arms/mm2$ to 30 $Arms/mm2$. By applying various current values into the motor FEM coil, torque response and corresponding flux linkage at various Ja points was investigated to observe the pattern of torque variation more clearly. For this design, the value of armature current as well as rms armature current is determined for the motor usage following the table of motor usage drawn in the Table 3.

Table 3 *Armature current density proposed design*

Armature Current Density, (J_a)	I_a peak	I_a rms
5	5.560	3.932
10	11.122	7.865
15	16.683	11.797
20	22.245	15.730
25	27.807	19.863
30	33.368	23.595

4.4 Maximum Flux vs Armature Current Density

The capability of motor can be indicated by torque, power and speed characteristic value. The efficiency of segmented stator FRM has been analysed in relation to the current density of the armature ranging from 0 $Arms/mm2$ to 30 $Arms/mm2$. The power ramped as the heat rose. The characteristics of fig.8 is that the maximum flux increases the armature current density increase proportional for the graphs. As seen in the following sub-section the overall U-phase flux interaction values for the proposed modular rotor FRM designs are about 1.0148 Wb at the different Ja.

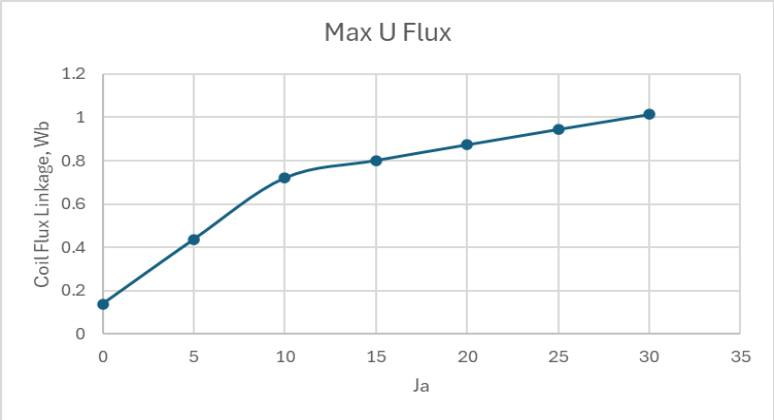

Fig. 8 *Flux vs Armature current density characteristic design SSFRM*

4.5 Power Losses and Efficiency

In motors, losses can actually be of two forms which is the copper losses (Pc) and the iron losses (Pi). The value of the torque against the speed graph for the SSFRM Design has fourteen points and it shows the following losses. Evaluations for the power losses and efficiency of the proposed design were made based on additional analysis of the project. High torque, moderate torque and low torque at high speed, moderate speed and low speed are shown in Fig. 9 at fourteen places.

The results of the design of SSFRM according to analysis often reveal less efficiency, more so at some operating conditions with copper loss being the main cause of the power loss rather than iron losses. This indicates it needs to optimise the magnetic design of a segmented motor of FRM and to run it at its best efficiency levels. The lower co-efficient of power and augmented iron losses at certain points suggest that they may be operating under something other than the most favourable conditions, which means that it may be possible to design the motor to reduce these losses which are inherent in some design of existing motors.

Evolution in Electrical and Electronic Engineering Vol. 6 No. 1 (2025) p. 76-84

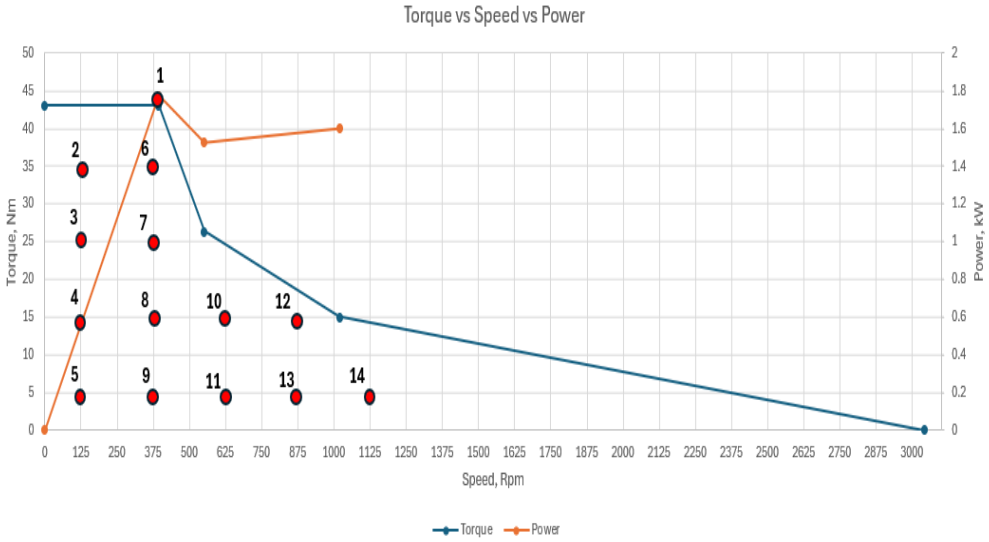

Fig. 9 *Points under the graph of torque vs. speed*

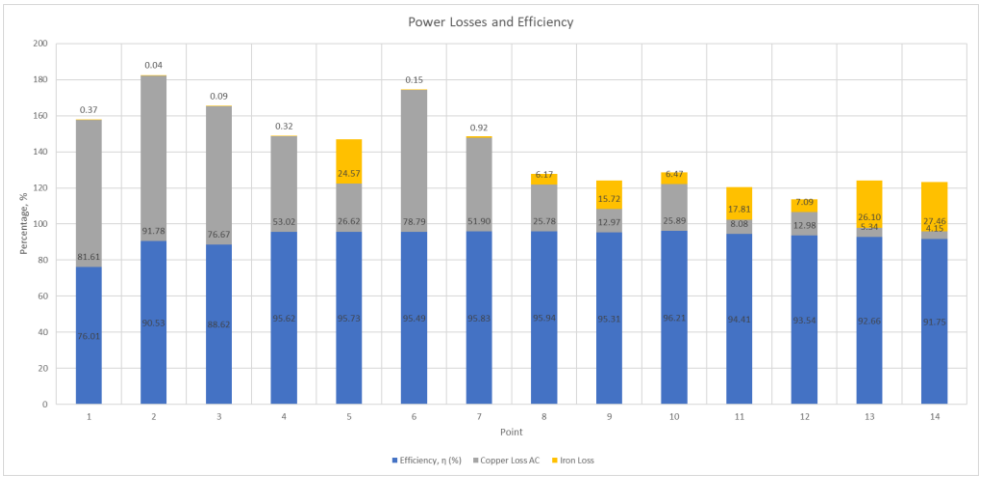

Fig. 10 *Power Losses and Efficiency at Operating Points for Design SSFRM*

4.6 General Performance for The SSFRM Design

The segmented stator FRM motor shows moderate power and torque performances but has high energy losses that lead to low efficiency. From a practical perspective it could stand an opportunity to be optimised for design for low iron and copper losses and high energy efficiency. These changes could make the motor more feasible for real world uses and that would increase its competitiveness. Table 4 shows the overall performance of the SSFRM designs for every criteria.

Table 4 *Comparison data of both proposed design*

Criteria	Propose Design
Efficiency, n	50.80 %
Max Torque, Nm	43.0534 Nm
Max Speed, rpm	1125 rpm
Max Power, kW	22.245 kW
Average Iron Loss, Pi	9.52 kW
Average Copper Loss, Pc	39.68 kW
Average Torque, Nm	18 Nm
Maximum U Flux, Wb	1.019 Wb
Average Speed, rpm	465.601 rpm
Average Power, kW	1.225 kW

5. Conclusion

The study focused on the design and performance of the four-segment permanent magnet flux reversal motor (SSFRM) with a 12-stator-slot, 16-pole configuration. This design enhanced torque and magnetic linkage while minimizing fault susceptibility and manufacturing complexity. The motor achieved a maximum torque of 43.05 Nm and an average torque of 18 Nm. Despite steady mechanical power output, efficiency was limited to 50.8% due to high copper losses (39.68 kW) and iron losses (9.52 kW). The maximum power delivery was 22.24 kW, with a tested flux linkage of 1.019 Wb and an average speed of 465.6 rpm. The findings highlight the potential of the segmental stator design but suggest further optimization to improve efficiency and reduce energy losses, encouraging future advancements for broader usability and higher performance.

Acknowledgement

The authors would also like to thank the Faculty of Electrical and Electronic Engineering, Universiti Tun Hussein Onn Malaysia for its support.

Conflict of Interest

Authors declare that there is no conflict of interests regarding the publication of the paper.

Author Contribution

The authors confirm contribution to the paper as follows: ***study conception and design:*** *Muhammad Hakim, Mahyuzie;* ***data collection:*** *Muhammad Hakim;* ***analysis and interpretation of results:*** *Muhammad Hakim, Mahyuzie;* ***draft manuscript preparation:*** *Muhammad Hakim, Mahyuzie. All authors reviewed the results and approved the final version of the manuscript.*

References

[1] Hwang, S. J., Lee, J., & Kim, S. J. (2021). Magnetic flux analysis and loss reduction in segmented stator permanent magnet motors. IEEE Transactions on Magnetics, 57(7), 1-10.
[2] Rahman, M. A., Islam, M. R., & Cho, Y. I. (2020). Optimization of cogging torque in permanent magnet machines using FEA tools. IEEE Transactions on Energy Conversion, 35(2), 1457-1465
[3] Tae Heoung Kim and J. Lee, "A Study of the Design for the Flux Reversal Machine," IEEE Transactions on Magnetics, vol. 40, no. 4, pp. 2053–2055, Jul. 2004, doi: https://doi.org/10.1109/tmag.2004.832488.
[4] C. Wang, S. Nasar, and I. Boldea, "Three phase flux reversal machine (FRM)," IEE Proc.—Elect. Power Appl., vol. 146, no. 2, pp. 139–146, Mar. 1999.
[5] Y. Gao, R. Qu, D. Li, J. Li, and L. Wu, "Design of three-phase flux reversal machines with fractional-slot windings," IEEE Trans. Ind. Appl., vol. 54, no. 4, pp. 2856–2864, Jul./Aug. 2016.
[6] Y. Gao, R. Qu, D. Li, J. Li, and G. Zhou, "Consequent-pole flux reversal permanent magnet machine for electric vehicle propulsion," IEEE Trans. Appl. Supercond., vol. 26, no. 4, Jun. 2016, Art. no. 5200105.
[7] C. X. Wang, I. Boldea, and S. A. Nasar, "Characterization of three phase flux reversal machine as automotive generator," IEEE Trans. Energy Convers., vol. 16, no. 1, pp. 74–80, Mar. 2001.
[8] R. Deodhar, S. Andersson, I. Boldea, and T. Miller, "The flux reversal machine: A new brushless doubly-salient permanent-magnet machine," IEEE Trans. Ind. Appl., vol. 33, no. 4, pp. 925–934, Jul./Aug.1997.
[9] Y. Gao, R. Qu, D. Li, and J. Li, "Torque performance analysis of three phase flux reversal machines for electric vehicle propulsion," in Proc. 2016 IEEE Conf. Expo Transp. Electrific. Asia-Pacific, Jun. 2016, vol. 1, pp. 296–301.
[10] Boldea, L. Zhang, and S. A. Nasar, "Theoretical characterization of flux reversal machine in low-speed servo drives-the pole-PM configuration," IEEE Trans. Ind. Appl., vol. 38, no. 6, pp. 1549–1557, Nov./Dec. 2002
[11] D. S. More and B. G. Fernandes, "Analysis of flux-reversal machine based on fictitious electrical gear," IEEE Trans. Energy Convers., vol. 25, no. 4, pp. 940–947, Dec. 2010.